Virology 428 (2012) 41–47

Contents lists available at SciVerse ScienceDirect

Virology

journal homepage: www.elsevier.com/locate/yviro

Disulfide-bond formation by a single cysteine mutation in adenovirus protein VI impairs capsid release and membrane lysis

Crystal L. Moyer, Glen R. Nemerow*

Department of Immunology and Microbial Sciences, The Scripps Research Institute, 10550 N. Torrey Pines Road, La Jolla, CA 92037, USA

ARTICLE INFO

Article history:
Received 7 February 2012
Returned to author for revisions
15 March 2012
Accepted 30 March 2012
Available online 17 April 2012

Keywords:
Adenovirus
Protein VI
Membrane penetration
Cell entry
Nonenveloped virus
Endosome

ABSTRACT

The internal capsid protein VI mediates adenovirus (AdV) endosome penetration during cell entry. Essential to this process is the release of protein VI from the AdV capsid and subsequent membrane targeting and insertion by the liberated VI molecules within the endocytic vesicle. In this study, we describe a human AdV (HAdV) substitution mutant (AdV VI-G48C) within the critical N-terminal amphipathic α-helical domain of protein VI. The VI-G48C virus displays altered capsid stability that impacts protein VI release, membrane disruption and virus infectivity. This is due in part to aberrant disulfide-bonding of protein VI molecules within the AdV particle. Our results provide insight into the structural organization of protein VI in the virus particle, as well as highlight the role of protein VI in cell entry.

Introduction

Nonenveloped virus (NEV) cell entry is a highly coordinated process that generally involves receptor binding, particle internalization, escape to the cytosol, and in some cases, subcellular trafficking to the nucleus. A critical step in this pathway is penetration of the limiting cellular membrane (i.e. plasma membrane, endosome, ER) to allow the viral genome access to the cell replication machinery. Generally, NEVs navigate this entry event via deployment of a previously shielded membrane lytic factor in response to specific host cell triggers (Tsai, 2007). Several different structural and functional classes of NEV lytic agents have been described and they have been shown to form pores or cause a gross rearrangement/disruption of the limiting cell membrane (Moyer and Nemerow, 2011).

For HAdV, the cell entry process is initiated via binding of the external fiber protein to a number of serotype-specific cellular receptors (reviewed in Sharma et al., 2009), followed by secondary engagement of the penton base with cell surface integrins (Wickham et al., 1993). Co-receptor engagement triggers the first of a series of disassembly steps within the AdV particle and is followed by uptake into clathrin-coated vesicles (Burckhardt et al., 2011; Lindert et al., 2009; Nakano et al., 2000). Once in the endocytic pathway, the low pH environment (Seth et al., 1984) is thought to further rearrange and dismantle the AdV capsid and results in release of the membrane-lytic internal protein VI (Greber et al., 1993; Wiethoff et al., 2005).

Protein VI is initially expressed as a 250 amino acid precursor (pVI) that is cleaved by the AdV-encoded protease at both the N- and C-termini, generating the mature protein VI (residues 34–239). In addition to its role in endosome lysis, protein VI has other functions in the AdV life cycle. At late stages of replication, protein VI chaperones hexon from the cytoplasm to the nucleus to facilitate particle assembly (Wodrich et al., 2003). A C-terminal peptide cleaved from pVI aids in capsid maturation, increasing AdV protease processivity by functioning as a co-factor (Mangel et al., 1993). During cell entry, VI also assists in AdV nuclear transport via microtubules (Wodrich et al., 2010). Though the precise structural location of the ~360 copies of protein VI within the AdV capsid (Lehmberg et al., 1999; van Oostrum and Burnett, 1985) remains to be defined, this capsid molecule is thought to function as a cement protein, providing increased stability to the particle shell (Liu et al., 2010; Reddy et al., 2010; Saban et al., 2006; Stewart et al., 1993; van Oostrum and Burnett, 1985).

The membrane lytic activity of protein VI is largely dependent upon a well-conserved N-terminal amphipathic α-helical domain (Fig. 1). Deletion of this region essentially abolishes membrane lytic activity by recombinant protein VI (Wiethoff et al., 2005). The current model for VI-mediated membrane lysis involves the planar insertion of the hydrophobic face of the helix into the target membrane, resulting in induction of positive curvature and ultimately large-scale membrane disruption (Maier et al., 2010).

We have recently described a panel of randomly generated AdV mutants within the amphipathic helical domain (Moyer et al., 2011). The study focused primarily on a single AdV protein VI point mutant (L40Q) that exhibited significant reductions in infectivity and endosome penetration. We now have systematically characterized

* Corresponding author. Fax: +1 858 784 8472.
E-mail address: gnemerow@scripps.edu (G.R. Nemerow).

0042-6822/$ - see front matter © 2012 Elsevier Inc. All rights reserved.
http://dx.doi.org/10.1016/j.virol.2012.03.024

a unique mutant from this panel, AdV VI-G48C (Fig. 1), which is also attenuated for infectivity and membrane disruption, albeit in a mechanistically distinct manner. The G48C mutation induces formation of disulfide-bonded dimers of protein VI within the AdV particle, altering capsid stability and protein VI exposure. This mutant reveals the likely oligomeric organization of protein VI within the virion and highlights the importance of protein VI in AdV infectivity and membrane disruption.

Results

The G48C mutation impairs virus infectivity

We previously described a method for generating recombinant adenoviruses with mutations in the protein VI amphipathic α-helical domain (Moyer et al., 2011). In this study, we investigated a unique mutation in protein VI (G48C) that impacts virus cell entry and infection. We first compared wild type and a previously characterized L40Q mutant, with AdV VI-G48C in a single-round infection assay as measured by gene delivery. All viruses showed a dose-dependent increase in infection as a function of input particles/cell (p/c) (Fig. 2A). We used the data from this experiment to calculate ID_{50} values for each virus and found that the G48C mutant required ~3-fold higher p/c than wild type AdV to achieve the same level of infection. The decrease in infectivity for the G48C mutant was not as drastic as that of the AdV VI-L40Q virus, which was 12-fold reduced compared to wild type virus. Nonetheless, the phenotype of the G48C mutation is distinct from that of L40Q, as described below.

We further assayed infectivity of the G48C mutant in an AdV plaque assay that measures viral replication, and show that the mutant generated ~3-fold less plaques than wild type AdV at 0.5 p/c (Fig. 2B), in good agreement with the data from the single-round infection (Fig. 2A). The L40Q virus was also reduced ~13-fold in this assay. Taken together, the results of these assays clearly indicate that the AdV VI-G48C mutant impairs virus infectivity.

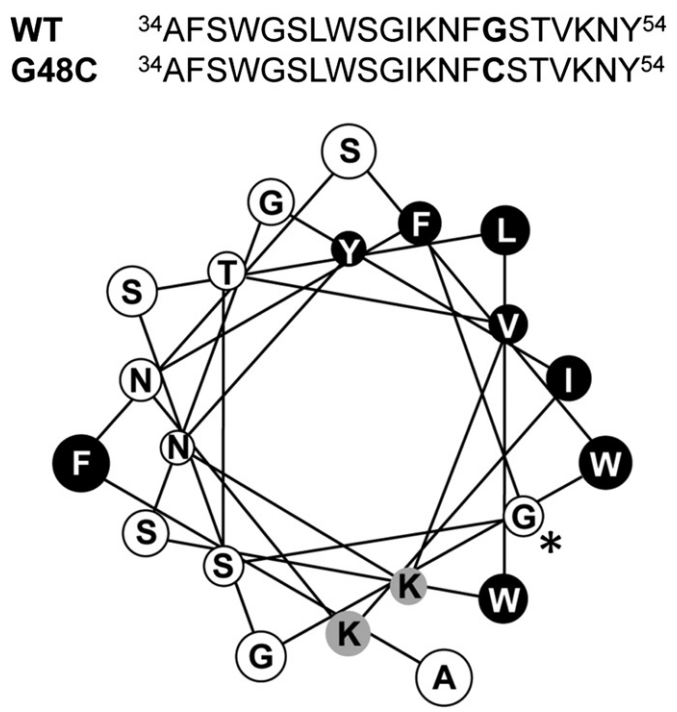

Fig. 1. Protein VI amphipathic α-helix. (Above) Residues 34–54 of the N-terminal amphipathic α-helix are shown as a linear sequence, with position 48 highlighted in bold face for the wild type and G48C proteins. (Below) The amphipathic α-helix is depicted as a helical wheel projection. Residue G48 is marked with an asterisk. Amino acids are shaded as follows: hydrophobic—black, polar—white, basic—gray.

Protein VI harboring the G48C mutation forms a dimer in the virus particle

To better understand why the G48C mutation negatively impacts infectivity, we first analyzed the protein composition of purified G48C mutant virus via SDS-PAGE under reducing conditions. Using gel densitometry, we observed no change in the total amount of protein VI incorporated into G48C particles when compared to wild type AdV (data not shown). In addition, we noted that pVI was fully cleaved to mature VI, suggesting that the G48C mutant VI retained the ability to act as a co-factor for the AdV protease (Mangel et al., 1993; Webster et al., 1993) and that capsid maturation proceeded normally.

However, the G48C mutation could affect the structural organization of protein VI within the capsid. In particular, the introduction of a cysteine residue in the VI molecule could cause disulfide bond formation with closely apposed protein VI molecules or with other capsid proteins within the virus particle. Therefore, we analyzed purified virus by SDS-PAGE and immunoblot for protein VI under reducing and non-reducing conditions (Fig. 3A). Wild type AdV showed a single band corresponding to monomeric protein VI (migrates as ~27 kDa) in samples treated with or without DTT. In contrast, protein VI from the G48C virus migrated as two distinct bands, corresponding to the expected molecular weights of a monomer and dimer (~54 kDa) in the

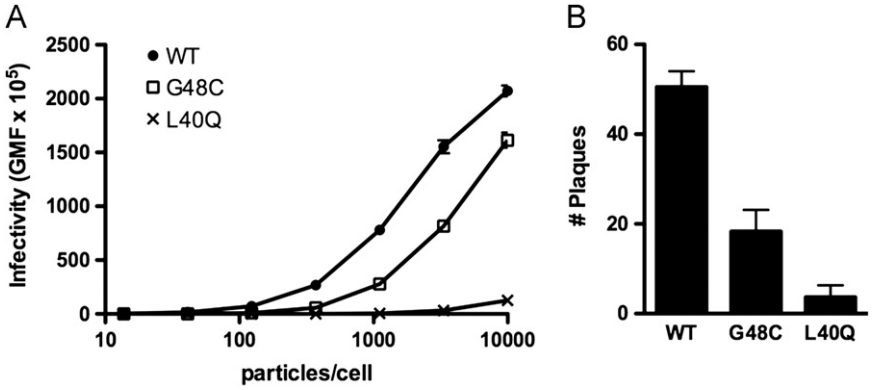

Fig. 2. Infectivity of the VI-G48C mutant virus. (A) A549 cells were infected with serial dilutions of the AdVs indicated. Infection (GFP expression) was measured 48 h pi with a Typhoon Fluorimager. The geometric mean fluorescence (GMF) ± SEM for triplicate samples is plotted. (B) 293β5 cells were infected with 0.5 particles/cell and overlaid with Avicel. After 72 h, the plates were imaged and the number of plaques/well was quantified. Data are the mean number of plaques/well ± SEM from triplicate wells.

non-reducing sample. Inclusion of DTT in the sample buffer completely converted protein VI to monomeric form. Using similarly prepared samples and gel densitometry analysis, we calculated the ratio of monomer:dimer to be approximately 1:1.4 (data not shown). From these analyses, we conclude that the G48C mutation enables a significant portion of the protein VI molecules to form homodimers within the virus particle.

To more fully explore the consequences of dimer formation on protein VI functions, we engineered the G48C mutation into the protein VI coding region comprised of residues 34–114 in a bacterial expression vector (VI114). The membrane lytic activity of this truncated form of protein VI is nearly identical to the full-length version of the protein (Maier et al., 2010). SDS-PAGE analysis of purified VI114 protein variants revealed that the G48C mutant migrated as a mixture of monomer and dimer under non-reducing conditions, while wild type and L40Q were strictly monomeric (Fig. 3B). As with the G48C virus, treatment of VI114-G48C with DTT converted all the protein VI to a monomeric species, demonstrating the dependence of this dimerization on intermolecular disulfide bonding. As expected, the L40Q mutant protein VI did not exhibit dimerization.

The G48C mutation alters capsid stability and restricts protein VI release

Release of protein VI from the interior of the HAdV capsid during cell entry is a critical step in productive infection (Greber et al., 1996; Smith and Nemerow, 2008). Therefore, we reasoned

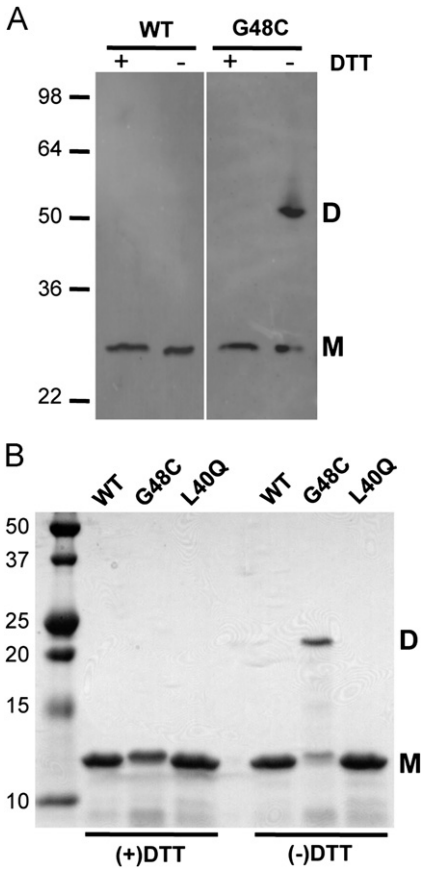

Fig. 3. Protein VI molecules are disulfide-linked in VI-G48C particles and purified protein. (A) Purified wild type or VI-G48C AdV were boiled in SDS sample buffer ± 2 mM DTT and analyzed by SDS-PAGE and western blot for protein VI. (B) affinity-purified recombinant VI114 proteins were boiled in SDS sample buffer ± 2 mM DTT, loaded on SDS-PAGE gels, and visualized with Simply Blue staining. Dimer (D) and monomer bands (M) are indicated in both panels.

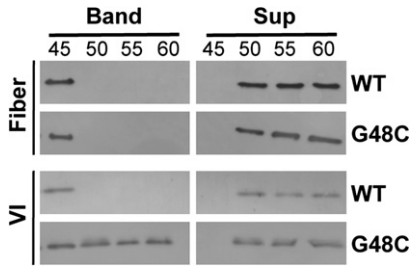

Fig. 4. Thermostability of AdV particles containing the G48C mutation. AdV was incubated at the indicated temperatures and the heat-disrupted particles were subjected to density gradient ultracentrifugation to separate core-associated (band) and released (sup) proteins as described in the Methods. Fiber and protein VI were visualized via immunoblot.

that dimerization of protein VI via disulfide bond formation within the virus particle could alter proper VI release from the capsid in the cell endosome. To test this hypothesis, we employed a well-characterized AdV thermostability assay designed to mimic AdV endosomal uncoating. Two AdV proteins, fiber and VI, were used as indicators of capsid dissociation following heating. Fiber protein, located on the exterior of the capsid at the five-fold vertices, is one of the first proteins to be released during cell entry. We observed that for both the wild type and G48C virions, fiber was released between 45 and 50 °C (Fig. 4). However, the pattern of protein VI release differed markedly between the wild type and G48C mutant. Protein VI release for the wild type virus paralleled fiber release, with full dissociation occurring between 45 and 50 °C. In contrast, protein VI from the G48C mutant was only partially liberated from the capsid at the same temperature range, while a significant portion (~50%) of the protein remained associated with the core even up to temperatures as high as 60 °C. These findings suggest that the release of G48C protein VI molecules from the capsid is more restricted than the WT protein, perhaps due to increased capsid stability, a situation that would impair endosome disruption and subsequent infection.

The G48C mutation alters VI membrane lytic activity

In order to directly examine whether the G48C mutation alters protein VI membrane lytic activity, we used an in vitro assay to assess protein VI-mediated liposome disruption mediated by heat-disassembled virions. A clear dose-dependent increase in membrane lytic activity was observed for wild type and mutant viruses (Fig. 5A). However, the data derived from the G48C and L40Q viruses revealed lower membrane disruption activity than that for wild type virions. Specific liposome lysis by AdV VI-G48C was 1.4- and 2.7-fold less than wild type virions at concentrations of 12.5 and 6.25 μg/ml, respectively. AdV VI-L40Q lytic activity was more severely attenuated than G48C, in good agreement with the infectivity data indicating that this virus is less infectious.

As the observed decrease in liposome lysis mediated by thermally dissociated AdV VI-G48C particles could be attributed to the partial defect in VI release following heat treatment at 50 °C, we next assessed the lytic activity of the purified VI114 proteins. We also observed a dose-dependent increase in lytic activity for each protein VI variant, with the two mutants being right-shifted compared to wild type (Fig. 5B). The reduction in membrane lysis for recombinant G48C was similar to that seen for the heat-disrupted virus, ranging from 1.7- to 4.8-fold at concentrations of protein from 1.6 to 0.4 μg/ml. L40Q again exhibited more attenuated lytic activity, with reductions compared to wild type protein between 3.9- to 10-fold over the same protein concentrations. Together, these results indicate that the

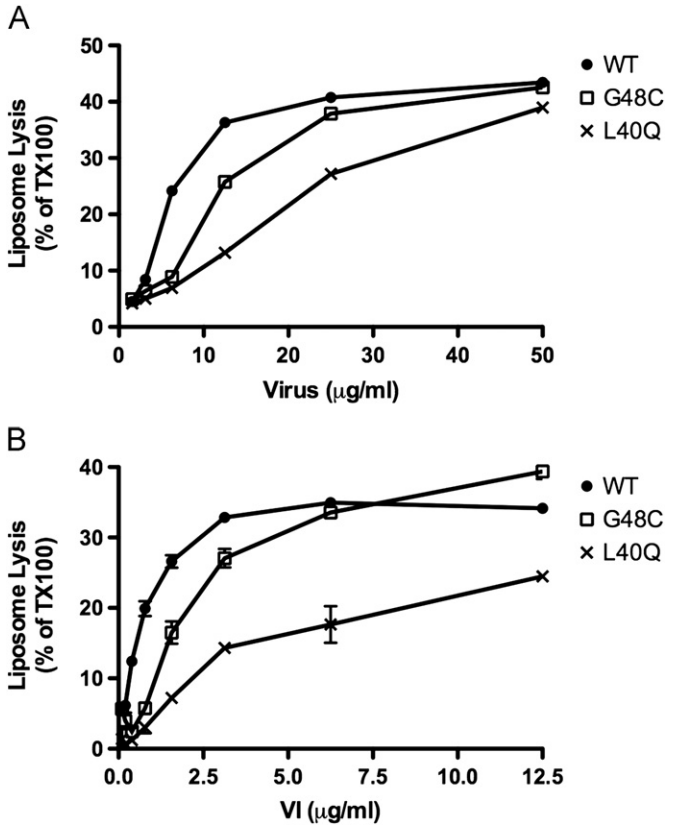

Fig. 5. G48C attenuates protein VI membrane lytic activity. Serial dilutions of heat-disrupted virus (A) or recombinant protein VI114 (B) at the indicated concentrations were mixed with liposomes and incubated at 37 °C. Liposome lysis (Sulfo B release) was monitored with a Tyhpoon Fluorimager. The mean percentage of specific lysis ± SEM relative to complete lysis in the presence of Triton X-100 is plotted. Data are from triplicate samples.

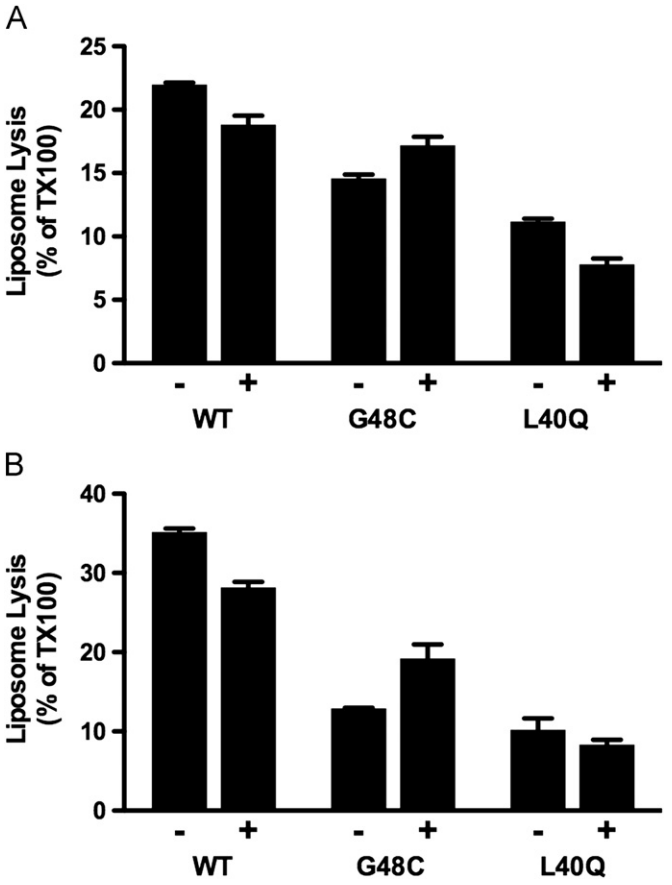

Fig. 6. Reduction of disulfide bonds partially restores G48C lytic activity. AdVs (A) or recombinant protein VI (B) were treated with (+) or without (−) 10 mM DTT before being assessed for liposome lysis activity as in Fig. 5.

decrease in virus infection induced by the G48C protein VI mutation is a consequence of both restricted capsid release and partially defective membrane disrupting activity.

DTT treatment partially restores VI lytic activity

Given the inherent decrease in membrane lytic activity of the disulfide bonded protein VI molecules, we next asked whether reduction of the disulfide bonds could restore membrane lytic activity to the G48C protein. DTT treatment modestly reduced membrane lytic activity of wild type and L40Q protein VI perhaps due to non-specific or off-target effects (Fig. 6). In contrast, the membrane lytic activity of heated virions and recombinant VI114-G48C (Figs. 6A and B, respectively) increased modestly following incubation with DTT. This small increase in membrane lytic activity was consistently observed in three independent experiments. Therefore, we conclude that disulfide bond formation not only restricts release of the membrane lytic protein from the viral capsid, but also impairs proper interaction with the host membrane that allows subsequent membrane lytic activity.

Discussion

Although our knowledge of endosome penetration by AdV has steadily improved over the past several years, we still lack a complete understanding of the structural and biochemical properties underlying this crucial cell entry step. The VI-G48C mutant AdV we have described in this study reveals details about protein VI organization within the AdV particle, as well as advances our understanding of membrane penetration.

Circular dichroism spectroscopic analysis has revealed that the N-terminal domain of protein VI (34–114) is >85% α-helix (Maier et al., 2010) and that an amphipathic α-helical segment (residues 34–54) contains the majority of membrane lytic activity (Wiethoff et al., 2005). Structural predictions indicate that the remaining C-terminal domain is largely disordered. Within the context of the AdV particle, there is no conclusive data on the structural organization of the ~360 molecules of protein VI. Biochemical (Matthews and Russell, 1994, 1995) and genetic (Wodrich et al., 2003) analyses are consistent with a direct interaction between protein VI and hexon. Additionally, X-ray crystallography and cryoelectron microscopy reconstructions of AdV particles assign density within the internal cavity of hexon trimers to protein VI (Liu et al., 2010; Perez-Berna et al., 2009; Reddy et al., 2010; Saban et al., 2006; Silvestry et al., 2009). While putative VI density is observed under every hexon, these structural techniques depend on icosahedral averaging to generate high resolution structural data; therefore, it remains unclear what proportion of hexons are associated with protein VI molecules and how VI is arranged. The symmetry mismatch (~360 copies of protein VI to 240 hexon trimers) obscures interpretation of the observed density, as stoichiometry calculations would indicate 1.5 molecules of protein VI per hexon trimer. Thus, the oligomeric state of protein VI in the virion remains an enigma, as well as its role in capsid stability and membrane damage. As revealed from the studies presented here, the formation of intermolecular disulfide bonds in the G48C mutant virus suggests that a subpopulation of individual VI molecules within the particle must be

in close enough proximity to form dimers, given that the average disulfide bond is approximately 2.02–2.04 Å in length (Petersen et al., 1999). Interestingly, chemical crosslinking (Chatterjee et al., 1985) and size-exclusion chromatography (Everitt and Philipson, 1974) studies with disrupted virions indicated that a portion of protein VI molecules in the capsid form dimers, further substantiating our findings. If protein VI were exclusively dimerized in the AdV capsid, we would expect nearly all protein VI molecules to be involved in intermolecular disulfide bonds in the G48C capsid. However, we observed that only ~58% dimer formation in the mutant. This finding is more consistent with trimers of protein VI molecules within the particle, a structural organization that would ideally lead to 66% dimer formation. Alternatively, protein VI molecules may exist in different oligomeric states depending on their association with quasiequivalent hexons that are in four distinct structural positions (i.e. a natural mixture monomer and dimer).

We did not observe a difference in protein VI incorporation into the virions during capsid maturation, suggesting that proper assembly occurs in the presence of VI dimers or that protein VI dimerization occurs post-assembly. Nevertheless, our studies clearly demonstrate a diminished ability of AdV bearing the G48C mutation to damage membranes and to infect cells. It is currently difficult to determine the relative contribution of reduced VI release from the capsid and decreased membrane rupture in the diminished AdV VI-G48C infectivity, but both are likely to contribute. There is currently no data on the number of protein VI molecules that must be released in the endosome to allow rupture and particle escape to the cytoplasm. However, a complete lack of protein VI exposure as occurs in a hyperstabilized temperature sensitive mutant of HAdV type 2 (*ts*1), abrogates endosome lysis and infection (Greber et al., 1996; Weber, 1976). In the case of the AdV VI-G48C mutant, roughly 50% of the protein VI molecules remain capsid associated upon heating, suggesting that protein VI release in the endosome may also be defective. In contrast to the *ts1* mutant, we did not observe a complete block in infection. Thus, we propose that endosome penetration requires the release of only a subset ($<50\%$) of protein VI molecules.

The G48C mutant also showed attenuation in membrane lytic activity independent of protein VI release. The current model for VI mediated endosome disruption involves membrane lysis via induction of positive curvature (Maier et al., 2010). Furthermore, previous studies have indicated that three tryptophan residues (minimally) within the N-terminal helical domain insert into the membrane (Maier et al., 2010; Moyer et al., 2011). Helical wheel modeling indicates that Gly48 resides on the hydrophobic face of the amphipathic α-helix (Fig. 1). Based on this structural model, disulfide formation has the propensity to impact proper VI membrane insertion, as it essentially reduces the molar equivalents of protein VI within endocytic vesicles by half. Maximal lytic activity of VI molecules would be reduced if dimerization shields these residues from normal membrane insertion. Furthermore, monomers of protein VI containing the G48C mutation, in the absence of disulfide bonding, also show modest defects in membrane lysis. Thus substitution of a larger polar amino acid at position 48 alone may be sufficient to perturb VI membrane lytic activity. Glycine residues, due to their small size, confer conformational flexibility to amphipathic helices that mediate membrane curvature (Drin et al., 2007). It is possible the G48C mutation diminishes the ability of protein VI to induce positive curvature, thereby decreasing lytic activity.

Overall, the work presented here provides important clues to the organization of protein VI within the AdV capsid and emphasizes the role of this capsid protein in cell entry and infection. Additional structural studies should provide a more mechanistic understanding of the effects of the G48C mutation on AdV infection and protein VI membrane lytic activity.

Materials and methods

Cell lines and viruses

A549 (ATCC) and 293β5 cells (Smith et al., 2010) were cultured in DMEM (Invitrogen) supplemented with 10% FBS. The generation of wild type and mutant AdVs used in this study have been previously described and are based on a BAC vector (pAd5-GFPn1) encoding the HAdV5 genome (Moyer et al., 2011; Wodrich et al., 2010). A CMV-driven EGFP reporter cassette replacing the E1/E3 region of HAdV5 generates a replication-defective virus in a non-complementing cell line (e.g. A549). AdVs were grown in complementing 293β5 cells and purified from cellular lysates by banding in cesium chloride density gradients, followed by dialysis into A195 buffer (Evans et al., 2004). Aliquots were flash frozen in liquid nitrogen and stored at -80 °C. Purified virus was boiled in SDS sample buffer ± 2 mM dithiothreitol (DTT) and analyzed by SDS-PAGE and immunoblot with a polyclonal antibody to protein VI. This antibody was generated by immunizing rabbits with a recombinant version of mature protein VI.

Single-round infection

A549 cells were infected with serial dilutions of wild type or mutant AdVs in DMEM in black 96-well plates (Corning Inc.) and incubated for 48 h at 37 °C in 5% CO_2. GFP fluorescence intensity was measured for each well with a Typhoon Fluorimager (GE Healthcare). Geometric mean fluorescence was plotted as a function of the input particles/cell. Nonlinear regression analysis with GraphPad Prism (GraphPad Software Inc, La Jolla, CA) was used to calculate the dose of virus required for 50% of maximal infection (ID_{50}) as reported in the text.

AdV plaque assay

293β5 cells plated in 12-well plates were infected with AdV (0.5 particles/cell) diluted in DMEM for 1 h at 37 °C with rocking. The media was removed and the cells were washed with PBS. Cells were overlaid with a mixture of 1.2% Avicel (FMC Corporation) and EMEM (Lonza Biowhittaker) supplemented with 5% FBS. The cells were incubated for 72 h at 37 °C. Monolayers were scanned with a Typhoon Fluorimager and plaques (GFP positive foci) were enumerated with ImageJ.

Thermostability assay for AdV uncoating

AdV thermostability was assessed using a protocol that is similar to that previously described (Moyer et al., 2011; Smith and Nemerow, 2008). Briefly, AdVs (1.5 μg) were heated to 45, 50, 55 or 60 °C for 10 min, loaded onto a 30–80% Histodenz (Sigma) discontinuous gradient and centrifuged in an SW55ti rotor (Beckman Colter) for 1.5 h at 209,000*g* (ave). Supernatant (top) and band (interface) fractions were boiled in SDS gel loading buffer containing 2 mM DTT. SDS-PAGE was followed by immunoblot with a polyclonal α-protein VI antibody or the monoclonal anti-fiber antibody, 4D2 (NeoMarkers, Lab Vision Corporation, Fremont, CA).

Recombinant VI114 purification

A construct encoding residues 34–114 of protein VI with a N-terminal 6x-histidine tag was cloned into pET15b (EMD

Biosciences). The G48C and L40Q point mutations were generated with site-directed mutagenesis using the primers:

G48C-F: 5′-AATTTCTGTTCCACCGTTAAG, G48C-R: 5′-GGTGGAACAGAAATTTTTAATG, L40Q-F: 5′-GCTGGGGCTCGCAGTGGAGCGGC, L40Q-R: 5′-GCTCCACTGCGAGCCCCAGCTGAAG.

Proteins were expressed in BL21(DE3)-RIPL (Stratagene) cells grown in Circle Grow media (MP Biomedicals) and induced with 1 mM IPTG. Cells were lysed with Bugbuster Protein Extraction Reagent (EMD Chemicals) supplemented with 1 mg/ml lysozyme (Sigma), 20 units/ml Benzonase (Novagen), 150 mM NaCl, EDTA-free protease inhibitor tablets (Roche), and 10 mM imidazole. The his-tagged proteins were further purified by affinity chromatography on Talon Cobalt resin (Clontech) and exchanged into 50 mM Tris–HCl/100 mM NaCl pH 8.0 by gel filtration on a HiLoad Superdex 16/60 S75 column using an AKTApurifier (GE Healthcare). Purified protein was boiled in SDS sample buffer $\pm$2 mM DTT and analyzed on SDS-PAGE gels stained with Simply Blue (Invitrogen).

Determination of VI membrane lytic activity in vitro

Lipid solutions in chloroform [1-palmitoyl,2-oleoylphosphatidylcholine (POPC) and 1-palmitoyl,2-oleoylphosphatidylserine (POPS)] were purchased from Avanti Polar Lipids. The lipids (75 POPC:25 POPS mol%, 1 mg total lipid) were dried under nitrogen and resuspended in 1 mL of 100 mM sulforhodamine B (SulfoB, Molecular Probes) dissolved in 25 mM HEPES, 150 mM NaCl buffer pH 7.5 (HBS). Uniform vesicles were generated by extrusion through 0.2 mm polycarbonate filters. Free dye was removed using a PD-10 desalting column (GE Healthcare) equilibrated with HBS.

Partial disassembly of AdV particles was achieved by heating to 50 °C to release protein VI from the interior of the virion. Serial dilutions of virus or recombinant VI114 protein in HBS at the concentrations indicated in Fig. 5 were mixed with liposomes (10 μl protein, 1 μl liposomes, 39 μl HBS). The samples were incubated at 37 °C for 20 min with rocking and SulfoB release was measured with a Typhoon Fluorimager at an excitation wavelength of 532 nm. Full liposome lysis was achieved by adding Triton X-100 to 0.5%. Specific liposome lysis was calculated with the following formula:

$$\%\text{SulfoB released} = 100 \times [(F_{\text{prot}} - F_{\text{bkgd}})/(F_{\text{det}} - F_{\text{bkgd}})]$$

where F_{prot} is the fluorescence intensity in the presence of AdV or VI114 protein, F_{bkgd} is the background fluorescence, and F_{det} is the fluorescence intensity in the presence of 0.5% Triton X-100.

The membrane lytic activity of DTT-treated viruses or VI114 recombinant protein was assayed by pre-incubation of virus (315 μg/ml) or protein (225 μg/ml) for 1 h or 30 min, respectively, at room temperature in the presence or absence of 10 mM DTT. Viruses were then heated to 50 °C to allow protein VI release. Samples were diluted to 25 μg/ml (AdV) or 1 μg/ml (VI114 protein) and processed in liposome lysis assays as described above.

Acknowledgments

This work was supported by NIH grants HL054352, EY011421 and EY017540 to G.R.N. This is manuscript #21640 from The Scripps Research Institute.

References

Burckhardt, C.J., Suomalainen, M., Schoenenberger, P., Boucke, K., Hemmi, S., Greber, U.F., 2011. Drifting motions of the adenovirus receptor CAR and immobile integrins initiate virus uncoating and membrane lytic protein exposure. Cell Host Microbe 10, 105–117.

Chatterjee, P.K., Vayda, M.E., Flint, S.J., 1985. Interactions among the three adenovirus core proteins. J. Virol. 55, 379–386.

Drin, G., Casella, J.F., Gautier, R., Boehmer, T., Schwartz, T.U., Antonny, B., 2007. A general amphipathic alpha-helical motif for sensing membrane curvature. Nat. Struct. Mol. Biol. 14, 138–146.

Evans, R.K., Nawrocki, D.K., Isopi, L.A., Williams, D.M., Casimiro, D.R., Chin, S., Chen, M., Zhu, D.M., Shiver, J.W., Volkin, D.B., 2004. Development of stable liquid formulations for adenovirus-based vaccines. J. Pharm. Sci. 93, 2458–2475.

Everitt, E., Philipson, L., 1974. Structural proteins of adenoviruses. XI. Purification of three low molecular weight virion proteins of adenovirus type 2 and their synthesis during productive infection. Virology 62, 253–269.

Greber, U.F., Webster, P., Weber, J., Helenius, A., 1996. The role of the adenovirus protease on virus entry into cells. Embo J. 15, 1766–1777.

Greber, U.F., Willetts, M., Webster, P., Helenius, A., 1993. Stepwise dismantling of adenovirus 2 during entry into cells. Cell 75, 477–486.

Lehmberg, E., Traina, J.A., Chakel, J.A., Chang, R.J., Parkman, M., McCaman, M.T., Murakami, P.K., Lahidji, V., Nelson, J.W., Hancock, W.S., Nestaas, E., Pungor Jr., E., 1999. Reversed-phase high-performance liquid chromatographic assay for the adenovirus type 5 proteome. J. Chromatogr. B Biomed. Sci. Appl. 732, 411–423.

Lindert, S., Silvestry, M., Mullen, T.M., Nemerow, G.R., Stewart, P.L., 2009. Cryo-electron microscopy structure of an adenovirus-integrin complex indicates conformational changes in both penton base and integrin. J. Virol. 83, 11491–11501.

Liu, H., Jin, L., Koh, S.B., Atanasov, I., Schein, S., Wu, L., Zhou, Z.H., 2010. Atomic structure of human adenovirus by cryo-EM reveals interactions among protein networks. Science 329, 1038–1043.

Maier, O., Galan, D.L., Wodrich, H., Wiethoff, C.M., 2010. An N-terminal domain of adenovirus protein VI fragments membranes by inducing positive membrane curvature. Virology 402, 11–19.

Mangel, W.F., McGrath, W.J., Toledo, D.L., Anderson, C.W., 1993. Viral DNA and a viral peptide can act as cofactors of adenovirus virion proteinase activity. Nature 361, 274–275.

Matthews, D.A., Russell, W.C., 1994. Adenovirus protein-protein interactions: hexon and protein VI. J. Gen. Virol. 75 (Part 12), 3365–3374.

Matthews, D.A., Russell, W.C., 1995. Adenovirus protein–protein interactions: molecular parameters governing the binding of protein VI to hexon and the activation of the adenovirus 23K protease. J. Gen. Virol. 76 (Part 8), 1959–1969.

Moyer, C.L., Nemerow, G.R., 2011. Viral weapons of membrane destruction: variable modes of membrane penetration by non-enveloped viruses. Curr. Opin. Virol. 1, 44–99.

Moyer, C.L., Wiethoff, C.M., Maier, O., Smith, J.G., Nemerow, G.R., 2011. Functional genetic and biophysical analyses of membrane disruption by human adenovirus. J. Virol. 85, 2631–2641.

Nakano, M.Y., Boucke, K., Suomalainen, M., Stidwill, R.P., Greber, U.F., 2000. The first step of adenovirus type 2 disassembly occurs at the cell surface, independently of endocytosis and escape to the cytosol. J. Virol. 74, 7085–7095.

Perez-Berna, A.J., Marabini, R., Scheres, S.H., Menendez-Conejero, R., Dmitriev, I.P., Curiel, D.T., Mangel, W.F., Flint, S.J., San Martin, C., 2009. Structure and uncoating of immature adenovirus. J. Mol. Biol. 392, 547–557.

Petersen, M.T., Jonson, P.H., Petersen, S.B., 1999. Amino acid neighbours and detailed conformational analysis of cysteines in proteins. Protein Eng. 12, 535–548.

Reddy, V.S., Natchiar, S.K., Stewart, P.L., Nemerow, G.R., 2010. Crystal structure of human adenovirus at 3.5 A resolution. Science 329, 1071–1075.

Saban, S.D., Silvestry, M., Nemerow, G.R., Stewart, P.L., 2006. Visualization of alpha-helices in a 6-angstrom resolution cryoelectron microscopy structure of adenovirus allows refinement of capsid protein assignments. J. Virol. 80, 12049–12059.

Seth, P., Fitzgerald, D.J., Willingham, M.C., Pastan, I., 1984. Role of a low-pH environment in adenovirus enhancement of the toxicity of a Pseudomonas exotoxin-epidermal growth factor conjugate. J. Virol. 51, 650–655.

Sharma, A., Li, X., Bangari, D.S., Mittal, S.K., 2009. Adenovirus receptors and their implications in gene delivery. Virus Res. 143, 184–194.

Silvestry, M., Lindert, S., Smith, J.G., Maier, O., Wiethoff, C.M., Nemerow, G.R., Stewart, P.L., 2009. Cryo-electron microscopy structure of adenovirus type 2 temperature-sensitive mutant 1 reveals insight into the cell entry defect. J. Virol. 83, 7375–7383.

Smith, J.G., Nemerow, G.R., 2008. Mechanism of adenovirus neutralization by human alpha-defensins. Cell Host Microbe 3, 11–19.

Smith, J.G., Silvestry, M., Lindert, S., Lu, W., Nemerow, G.R., Stewart, P.L., 2010. Insight into the mechanisms of adenovirus capsid disassembly from studies of defensin neutralization. PLoS Pathog. 6, e1000959.

Stewart, P.L., Fuller, S.D., Burnett, R.M., 1993. Difference imaging of adenovirus: bridging the resolution gap between X-ray crystallography and electron microscopy. Embo J. 12, 2589–2599.

Tsai, B., 2007. Penetration of nonenveloped viruses into the cytoplasm. Annu. Rev. Cell Dev. Biol. 23, 23–43.

van Oostrum, J., Burnett, R.M., 1985. Molecular composition of the adenovirus type 2 virion. J. Virol. 56, 439–448.

Weber, J., 1976. Genetic analysis of adenovirus type 2 III. Temperature sensitivity of processing viral proteins. J. Virol. 17, 462–471.

Webster, A., Hay, R.T., Kemp, G., 1993. The adenovirus protease is activated by a virus-coded disulphide-linked peptide. Cell 72, 97–104.
Wickham, T.J., Mathias, P., Cheresh, D.A., Nemerow, G.R., 1993. Integrins alpha v beta 3 and alpha v beta 5 promote adenovirus internalization but not virus attachment. Cell 73, 309–319.
Wiethoff, C.M., Wodrich, H., Gerace, L., Nemerow, G.R., 2005. Adenovirus protein VI mediates membrane disruption following capsid disassembly. J. Virol. 79, 1992–2000.
Wodrich, H., Guan, T., Cingolani, G., Von Seggern, D., Nemerow, G., Gerace, L., 2003. Switch from capsid protein import to adenovirus assembly by cleavage of nuclear transport signals. Embo J. 22, 6245–6255.
Wodrich, H., Henaff, D., Jammart, B., Segura-Morales, C., Seelmeir, S., Coux, O., Ruzsics, Z., Wiethoff, C.M., Kremer, E.J., 2010. A capsid-encoded PPxY-motif facilitates adenovirus entry. PLoS Pathog. 6, e1000808.